Cell

A Mutant-p53/Smad Complex Opposes p63 to Empower TGFβ-Induced Metastasis

Maddalena Adorno,[1,8] Michelangelo Cordenonsi,[1,8] Marco Montagner,[1] Sirio Dupont,[1] Christine Wong,[2] Byron Hann,[2] Aldo Solari,[3] Sara Bobisse,[4] Maria Beatrice Rondina,[4] Vincenza Guzzardo,[5] Anna R. Parenti,[5] Antonio Rosato,[4,6] Silvio Bicciato,[6,7] Allan Balmain,[2] and Stefano Piccolo[1,*]

[1]Department of Histology, Microbiology and Medical Biotechnologies, University of Padua School of Medicine, viale Colombo 3, 35100 Padua, Italy
[2]Cancer Research Institute, University of California, San Francisco, 2340 Sutter Street, San Francisco, CA 94115, USA
[3]Department of Chemical Engineering Processes, University of Padua, via F. Marzolo 9, 35131, Padua, Italy
[4]Department of Oncology and Surgical Sciences and Istituto Oncologico Veneto, University of Padua, via Gattamelata 64, 35126 Padua, Italy
[5]Department of Medical Diagnostic Science and Special Therapies, Section of Pathology, University of Padua, viale Gabelli 2, 35126 Padua, Italy
[6]Istituto Oncologico Veneto, via Gattamelata 64, 35126 Padua, Italy
[7]Department of Biomedical Sciences, University of Modena and Reggio Emilia, via G. Campi 287, 41100, Modena, Italy
[8]These authors contributed equally to the work
*Correspondence: piccolo@civ.bio.unipd.it
DOI 10.1016/j.cell.2009.01.039

SUMMARY

TGFβ ligands act as tumor suppressors in early stage tumors but are paradoxically diverted into potent prometastatic factors in advanced cancers. The molecular nature of this switch remains enigmatic. Here, we show that TGFβ-dependent cell migration, invasion and metastasis are empowered by mutant-p53 and opposed by p63. Mechanistically, TGFβ acts in concert with oncogenic Ras and mutant-p53 to induce the assembly of a mutant-p53/p63 protein complex in which Smads serve as essential platforms. Within this ternary complex, p63 functions are antagonized. Downstream of p63, we identified two candidate metastasis suppressor genes associated with metastasis risk in a large cohort of breast cancer patients. Thus, two common oncogenic lesions, mutant-p53 and Ras, selected in early neoplasms to promote growth and survival, also prefigure a cellular set-up with particular metastasis proclivity by TGFβ-dependent inhibition of p63 function.

INTRODUCTION

Cancer progression is a multistep process involving the accumulation of genetic and epigenetic changes in several genes. Still, how distinct defects cooperate to generate a metastatic tumor remains a long-standing unanswered question in cancer biology.

The fact that specific gene-sets, or signatures, already expressed in primary tumors have been found predictive for metastasis, has led to the proposal that metastatic proclivity might be intimately wired to the same aberrant genetic pathways that control tumorigenesis in the primary tumor (Bernards and Weinberg, 2002).

One of the most frequent genetic lesions in human tumors is mutation of the p53 tumor suppressor, which acts as transcription factor to promote cytostasis, apoptosis and genome integrity. More than 80% of p53 alterations are missense mutations that lead to the synthesis of a stable but transcriptionally deficient protein (Soussi and Beroud, 2001). Why do tumor cells retain a disabled tumor suppressor, rather than losing it for good? An important step in answering this question has been the generation of mutant-p53 knockin mice (Lang et al., 2004; Olive et al., 2004). Remarkably, tumors emerging in these models display aggressive and metastatic traits that are never detected in tumors developing in a *p53* null background. This is supported by molecular epidemiology data in humans, showing that mutant-p53 expressing tumors are aggressive and associated to poor-prognosis (Sorlie et al., 2001; Soussi and Beroud, 2001).

Intriguingly, activating mutations in the Ras signaling pathway appear critical for the malignant phenotypes of mutant-p53 (Caulin et al., 2007; Hingorani et al., 2005). Thus, p53 mutation, in concert with oncogenic Ras, leads to a gain of molecularly undefined properties that render mutant-p53 a dominant prometastatic factor. Whether this entails the intersection with other pathways involved in neoplastic transformation is unknown.

TGFβ/Smad signaling plays a central role for tumorigenesis of several epithelia, paradoxically switching from tumor suppressor to promoter of metastasis during cancer progression (Derynck et al., 2001). Here we present evidence of a TGFβ-initiated intracellular cascade specifically relevant in advanced tumor cells for metastasis. We show that mutant-p53 expression is required for sustaining TGFβ proinvasive responses and metastatic spread in vivo. Moreover, we shed light on the enigmatic nature of the prometastatic switches of mutant-p53 and TGFβ by showing that these converge on the same mechanism: Ras-activated mutant-p53 and TGFβ conspire to oppose the activity of the p53 family member p63. p63 is a master gene for normal epithelial stem cells, protecting them from apoptosis and coordinating their differentiation (Deyoung and Ellisen, 2007). Here we show

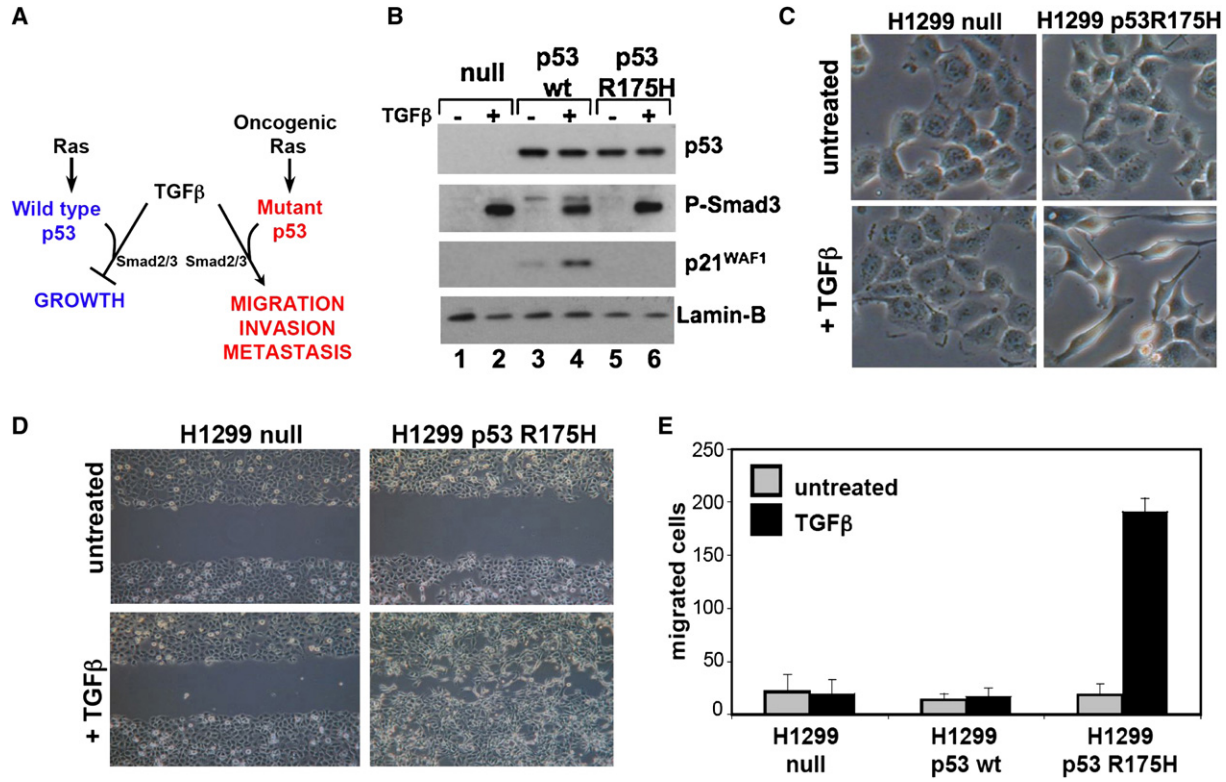

Figure 1. Mutant-p53 Expression Promotes TGFβ Promigratory Responses

(A) Schematic representation of our starting hypothesis.

(B) Western blot of H1299 cell lysates: parental, i.e., lacking p53 expression (null), reconstituted with wild-type p53 (p53 wt) or mutant-p53 (p53 R175H). Lamin-B is a loading control. Control RNA levels are shown in Figure S1B.

(C) Effect of TGFβ (5 ng/ml of TGFβ for 24 hr) on the morphology of H1299 cells.

(D) Wound healing assays of H1299 cells showing effect the mutant-p53 on TGFβ-driven migration (pictures taken after 30 hr).

(E) H1299 cells were seeded on transwell membranes. Where indicated, cells were treated with TGFβ. The graphs show the number of cells migrated through the transwell after 16 hr. Data are represented as mean and SD.

a role for p63 in metastasis protection that is disabled by the quantitative physical incorporation of p63 into a ternary protein complex together with mutant-p53 and TGFβ activated Smads. Finally, we also unveiled, and functionally validated, two genes regulated by this pathway that may be used as efficient prognostic tool in clinical settings.

RESULTS

Mutant-p53, but Not Wild-Type p53, Empowers a TGFβ Promigratory Response

We sought to compare the effects of wild-type and mutant-p53 on the cellular response to TGFβ (Figure 1A). To this end, we used *p53* null H1299 cells stably reconstituted with inducible expression vectors coding for wild-type human p53 or the hot-spot p53R175H mutant allele. The two cell populations expressed p53 proteins at similar levels and retained similar responsiveness to TGFβ, as judged by activation of P-Smad3 and of a synthetic reporter of Smad activity (pCAGA12-lux) (Figure 1B and Figure S1A available with this article online).

In agreement with previous findings, reconstitution of H1299 cells with wild-type p53 rescued the ability of TGFβ to induce $p21^{WAF1}$ and growth arrest (Figure 1B and data not shown, see Cordenonsi et al., 2007). In contrast, reconstitution with mutant-p53 was ineffective in this respect (Figure 1B). TGFβ treatment of H1299 cells bearing p53R175H caused instead a strikingly different phenotype, as cells shed their cuboidal epithelial shape and acquired a more mesenchymal phenotype, characterized by a number of dynamic protrusions, such as filopodia and lamellipodia (Figure 1C). These were not present in parental cells or in cells reconstituted with wild-type p53 (Figure 1C and data not shown). To examine if expression of mutant-p53 also conferred migratory properties to cells receiving TGFβ, we used a wounding assay, in which cells are induced to migrate into a wound created by scratching confluent cultures with a pipette tip. After TGFβ treatment, while parental (p53 null) or wild-type p53 reconstituted H1299 cells had migrated poorly, p53R175H expressing cells almost completely invaded the wound (Figure 1D and data not shown). As an independent mean of measuring cell motility, we also carried out transwell-migration assays. Figure 1E shows that expression of mutant-p53, but not of wild-type p53, parallels with the acquisition of a TGFβ promigratory response.

These data establish p53 as the only known Smad regulator whose mutational status can impart two profoundly different

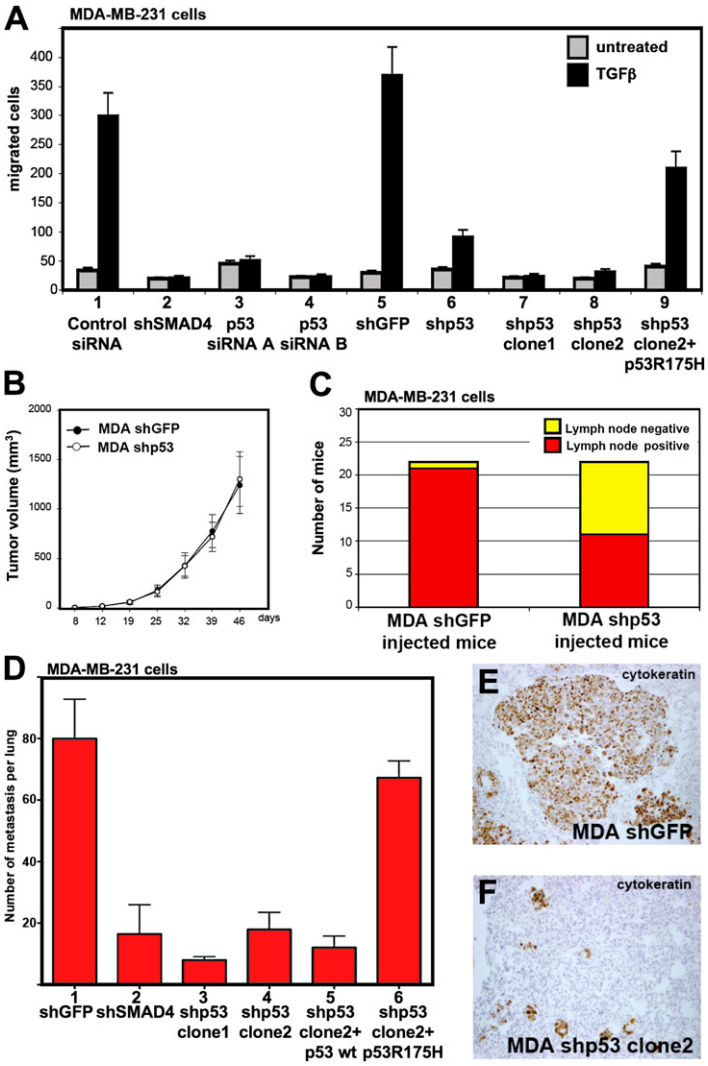

Figure 2. Mutant-p53 Is Required for TGFβ-Driven Invasion and Metastasis in Breast Cancer MDA-MB-231 Cells

(A) Transwell assay for TGFβ dependent migration of MDA-MB-231 cell lines. TGFβ was used at 5 ng/ml. This response depends on canonical Smad signaling, as attested by blockade of migration ensuing Smad4 depletion (compare lanes 1 and 2 and see also Figure S2B). Endogenous mutant-p53 is required for this response as validated by two independent siRNA sequences (A and B, respectively, lanes 3 and 4). The sequence corresponding to siRNA-B was cloned in pSUPER-Retro and used for stable p53 interference. We tested the whole population of positive transfectants (lane 6) or two independent clones (lanes 7 and 8). TGFβ-dependent migration of clone 2 is rescued by infection with a lentiviral vector coding for siRNA-resistant mutant-p53 (R175H, lane 9). Controls for p53 and Smad4 depletions are shown in Figure S2A. Data are represented as mean and SD.

(B and C) SCID mice were injected in the fat pad with MDA shGFP or MDA shp53 cells. (B) The rate of primary tumor growth was similar between the two cell populations. Data are represented as mean and SD (C) Number of mice scored positive for lymphonodal metastasis. To quantify metastatic spread, we monitored the colonization of controlateral lymph nodes, a read-out of systemic disease in human breast cancers (Sobin and Wittekind, 2002).

(D, E, and F) Lung colonization assays after tail vein injection of MDA-MB-231 cell lines (1×10^6 cells/mouse). (D) Total number of lung metastatic nodules in individual mice was counted on serial histological sections. Lane 1: control (shGFP) cells (n = 20). Lane 2: canonical Smad signaling is required for MDA-MB-231 lung metastasis as revealed by the inhibitory effect of Smad4 depletion (n = 9). Lanes 3 and 4: impaired metastasis in two independent shp53 clonal cell lines (clone 1 and 2, siRNA sequence B, see Figure 2A). Clone1, n = 10; clone 2, n = 21. Similar result was obtained by depletion of mutant-p53 with siRNA sequence A (Figure S2E). Lanes 5 and 6: effect of reconstitution with wild-type (n = 10) and mutant-p53 (R175H, n = 12). Panels show representative immunohistochemistry for human cytokeratin in sections of lungs from mice injected with MDA shGFP (E) or MDA shp53 (F). Data are represented as mean and SD.

interpretations to TGFβ signal, being able to switch the cellular responses from tumor suppressive, supported by wild-type p53 (Cordenonsi et al., 2003, 2007), to promalignant, promoted by mutant-p53.

Mutant-p53 Is Required for TGFβ-Driven Invasion and Metastasis in Breast Cancer Cells

Our data link the gain of mutant-p53 to TGFβ induced epithelial plasticity and migration, phenotypes whose emergence is critical for TGFβ invasive properties (Derynck et al., 2001). However, the actual requirement for these effects of mutant-p53 endogenously expressed in metastatic cancer cells remained a key unanswered issue. To address this, we knocked down endogenous mutant-p53 (p53R280K, Table S1) in MDA-MB-231 cells, a well-established model of invasive breast cancer. In transwell-migration assays, TGFβ triggered a Smad-dependent promigratory response in these cells (Figures 2A and S2B). Remarkably, this response was lost in mutant-p53-depleted cells (Figure 2A). Once embedded in a drop of Matrigel, MDA-MB-231 cells display a TGFβ dependent scattering, extracellular matrix degradation and migration (Figures S2C and S2D), recapitulating in vivo invasiveness. We found that mutant-p53 expression is required for these activities. These data suggest that, at least in vitro, mutant-p53 and TGFβ jointly control cell shape and invasiveness of breast cancer cells.

Multiple evidences indicate that the metastatic spread of MDA-MB-231 cells in vivo is under control of autocrine TGFβ (Table S1). To test if mutant-p53 is relevant for TGFβ promoted malignant behaviors in vivo, we injected control (shGFP) or stably mutant-p53 depleted (shp53) MDA-MB-231 cells into the mammary fat pad of immunocompromized mice. The two cell populations grew at similar rate in vitro (data not shown) and formed primary tumors at similar rates and size in vivo (Figure 2B), indicating that high levels of mutant-p53 in MDA-MB-231 cells are not essential for proliferation or primary tumor formation. Six weeks after implantation, mice were sacrificed and examined for presence of metastatic lesions. Orthotopically injected MDA-MB-231 are poorly metastatic to the lung, but efficiently metastasize to the lymph nodes. Strikingly, depletion of mutant-p53 drastically reduced the number of lymph node

metastases when compared to the control cells, as only one out of 22 mice injected with the shGFP cells scored negative for lymphonodal metastasis, whereas 10 out of 22 of mice carrying the shp53-depleted tumors remained metastasis-free (Figure 2C).

To confirm these results implicating mutant-p53 in invasiveness in vivo, we injected control and shp53-MDA-MB-231 intravenously into nude mice. Mutant-p53 is required for lung colonization, as two independent clones of shp53-MDA-MB-231 cells displayed overt reduction of metastatic nodules in number and size (Figures 2D–2F). While control cells massively invaded the lung parenchyma, small nodules of shp53-cells remained confined perivascularly (Figure S2F). As specificity control, metastatic behavior of shp53-MDA-MB-231 cells is rescued by adding back siRNA insensitive mutant-p53, but not wild-type p53 (Figure 2D, compare lanes 4, 5, and 6).

Taken together, the data suggest that mutant-p53 expression plays a crucial role in canalizing TGFβ responsiveness for efficient metastatic spread.

p63 Is Downstream of Mutant-p53 and Opposes TGFβ-Induced Malignant Responses

Knockin mice expressing mutant-p53 (*p53+/R172H* or *p53+/R270H*) develop metastatic carcinomas, a phenotype never observed in mice simply lacking one *p53* allele (*p53+/−*) (Lang et al., 2004; Olive et al., 2004). Intriguingly, loss of one allele of *p63* or *p73* similarly endows *p53+/−* tumors with metastatic properties (Flores et al., 2005). The parallel between loss of p63/p73 and gain of mutant-p53 is compatible with mutant-p53 acting as a restraining factor for the activity of its family members. Interestingly, loss of p63 or p73 fosters progression, but in distinct tumor spectra, with loss of p63 specifically promoting the emergence of metastatic cancers in stratified epithelia (Flores et al., 2005), that is, tumor types characterized by a clear promalignant-switch in TGFβ responses (Derynck et al., 2001).

These hints prompted us to test the role of p63 in cell migration and invasion induced by TGFβ. Transient transfection of p63 (both TA or ΔNp63α isoforms) caused a marked inhibition of TGFβ-induced transwell migration (Figure 3A). Conversely, siRNA-mediated depletion of p63 in parental H1299 cells empowers TGFβ-induced migration, phenocopying gain of mutant-p53 (Figure 3B). We then tested the epistatic relationships between mutant-p53 and p63. Crucially, loss of p63 leads to a remarkable rescue of TGFβ promigratory and proinvasive properties in p53-depleted MDA-MB-231 cells (Figure 3C, lanes 3 and 4). To functionally support this notion in vivo, we stably antagonized endogenous p63 activity using a dominant-negative protein, termed p63DD, consisting of EGFP fused in frame with the p63 tetramerization domain (Figures S4A and S4B). We used a lentiviral delivery system to stably introduce p63DD in shp53 MDA-MB-231 cells. Remarkably, p63 inactivation substantially rescues lung colonization in mutant-p53-depleted cells (Figure 3E). Taken together, the evidences in vitro and in vivo suggest that TGFβ uses mutant-p53 to surpass the barrier that p63 raises against TGFβ-induced malignant cell responses (Figure 3D).

If p63 inhibition by mutant-p53 and TGFβ allows the exploitation of TGFβ proinvasive properties in metastatic cells, then experimental downregulation of p63 in non-invasive tumors might unleash a TGFβ-dependent transition toward more aggressive cell phenotypes. To test this, we used non-invasive skin squamous carcinoma B9 cells (Oft et al., 2002). After transfection of p63-siRNA, B9 cells displayed loss of epithelial and gain of mesenchymal traits (Figures 3F–3H). This shift was inhibited by blocking TGFβ receptor I activity with SB431542, indicating the reliance on endogenous TGFβ signaling. To investigate the role of p63 in vivo, we stably transduced p63DD in B9 cells and, as a control, in H11 aggressive spindle cells (expressing extremely low levels of p63, data not shown). Cells bearing p63DD or only GFP (as control) were injected sub-cutaneously into nude mice, and their growth as xenograft tumors was observed. While expression of p63DD had little effect on tumor growth and morphology of H11 cells (data not shown), tumors emerging from p63DD engineered B9 cells displayed an accelerated growth, decreased differentiation and acquisition of a spindle phenotype with increased stromal invasion (Figures 3I and 3J).

A TGFβ- and Ras-Dependent Ternary Complex

We next sought to address the mechanism by which TGFβ controls p63 through mutant-p53. Previous work has shown that, at the biochemical level, the recombinant core domain of some mutant-p53 proteins, but not of wild-type p53, binds and inhibits p63 by masking its DNA binding domain (Gaiddon et al., 2001; Strano et al., 2002). However, several observations suggest that this biochemical model is an oversimplification, that misses at least one essential component. Indeed, to be effective as an antagonist, mutant-p53 should be able to quantitatively titrate p63; in contrast, there is scant evidence that such interaction can effectively occur in vivo at physiological concentrations of these proteins (Caulin et al., 2007, and see below). Moreover, stratified epithelia almost exclusively express ΔNp63, an isoform per se unable to complex mutant-p53 (Gaiddon et al., 2001).

We tested if Smads might be the missing link between mutant-p53 and p63 inactivation. For this, we first immunoprecipitated endogenous mutant-p53 from HACAT keratinocytes (carrying the p53H179Y/R282W mutations, Table S1). Co-precipitating proteins were revealed by Western blotting. In lysates of untreated cells we could detect only a weak interaction between p63 and mutant-p53, but this association was massively augmented in the presence of TGFβ signaling (by more than 20-fold; Figure 4A, compare lanes 2 and 3). Crucially, endogenous Smads are essential for mutant-p53/p63 complex formation, becoming this undetectable upon transfection of siRNA against Smad2/3 (Figure 4A, compare lane 3 and 4). These findings suggest that TGFβ signaling is an essential determinant for mutant-p53 to complex its family member p63. In an alternative experimental set-up, coimmunoprecipitation using anti-Smad2 antibodies reveals Smad2 associated with p63 and mutant-p53 (Figure 4B); yet, while the interaction of Smad2 with p63 is to a large extent independent from mutant-p53 (Figure 4B, lane 3), Smad binding to mutant-p53 requires p63 (Figure 4B, lane 4), suggesting that mutant-p53 preferentially associates to a preassembled p63/Smad2 scaffold in these cells. Together, these biochemical data indicate the formation of a TGFβ-induced ternary complex between endogenous p63, mutant-p53 and Smads.

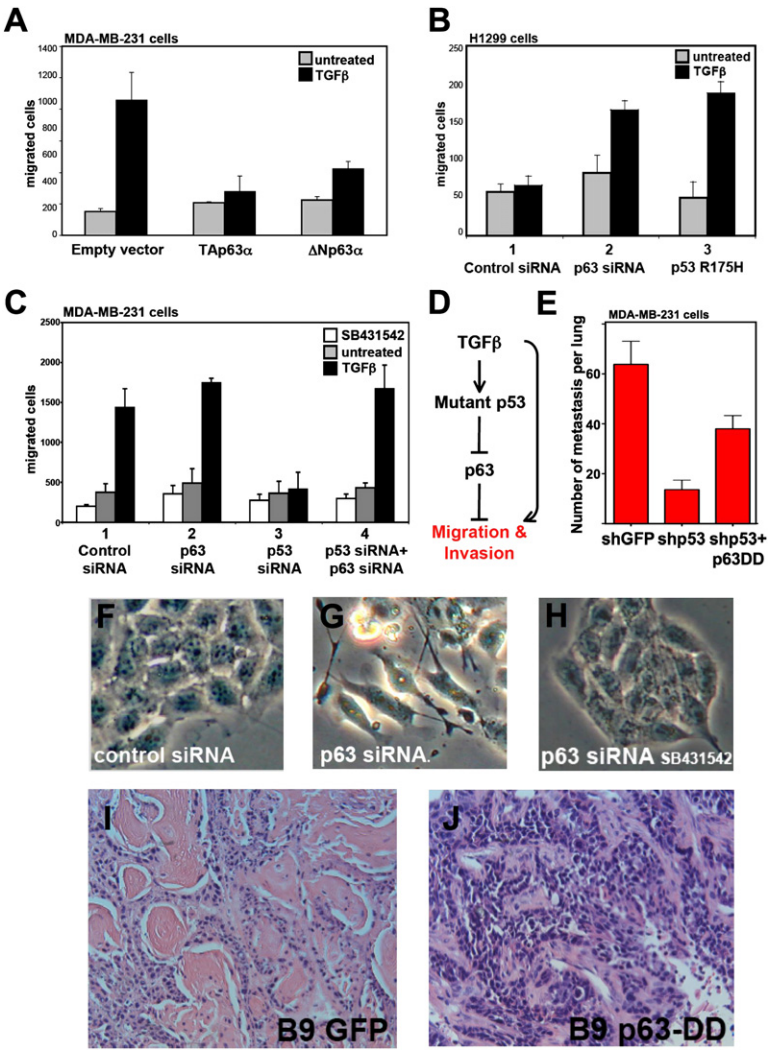

Figure 3. p63 Opposes TGFβ-Driven Migration

(A) Transwell assay of MDA-MB-231 transiently transfected with the indicated p63 expression vectors. p63 expression levels are shown in Figure S3A. Data are represented as mean and SD.

(B) Loss of p63 confers migratory abilities to H1299 cells in response to TGFβ, phenocopying the gain of mutant-p53. Graphs show quantification of cells migrated into a defined wound area 24 hr after cell scraping. Data are represented as mean and SD.

(C) Transwell migration assay of MDA-MB-231 after transfection of indicated siRNAs. TGFβ induced migration is impaired by loss of mutant-p53, but is rescued in cells with dual depletion of both p53 and p63. The experiment was repeated in matrigel-coated transwell filters to monitor invasiveness (Figure S3C). Similar results were obtained using an siRNA targeting a different region of p63 mRNA (Figure S3D). The efficiency of p53 and p63 depletion is shown in Figure S3B. Note that once p63 is depleted, mutant-p53 becomes dispensable - and TGFβ proficient - for induction of cell migration (see diagram in [D]). Figure S4C provides independent evidences for this epistasis by using a p63 dominant-inhibitor, p63DD. Data are represented as mean and SD.

(D) Model of the epistatic relationships between TGFβ, mutant-p53 and p63.

(E) Functional inactivation of p63 by overexpression of p63DD in shp53MDA-MB-231 clone 2 (as in Figure 2D) rescues lung metastastic colonization in tail vein assays ($n = 8$, 1×10^6 cells/mouse). Data are represented as mean and SD.

(F, G, and H) Morphology of B9 squamous cell carcinoma 48 hr after the indicated siRNA transfection. Note that control cells form an epithelial monolayer (F) whereas p63 depletion leads to a mesenchymal morphology (G); similar results were obtained by overexpression of p63DD (data not shown). This phenotype can be reverted by treatment with SB431542 (H) and is primed by exogenous TGFβ (data not shown). Efficacy of p63 depletion is shown in Figure S4D.

(I and J) Representative hematoxylin-eosin stainings on paraffin sections of tumors resulting after subcutaneous injection of engineered B9 cells. While control (GFP-transduced) cells formed well-differentiated tumors with keratin pearls (I), p63-DD expressing tumors were less differentiated and acquired invasive traits (J).

A wealth of evidence in cancer cells and animal models clearly indicates that metastasis requires the combination of elevated TGFβ and Ras signaling, but the mechanisms of this intersection remain unclear (Grunert et al., 2003). Interestingly, we previously showed that the same pathways are involved in mesoderm development in *Xenopus* embryogenesis: in that case, however, it is wild-type p53 that serves as link between Smad and RTK signaling (Cordenonsi et al., 2007). These precedents prompted us to test if oncogenic Ras may feed on mutant-p53 for the formation of the ternary complex. We first wished to address this in a cellular context free from the multiple genetic changes that typically characterize cancer cell lines. For this, we used MEFs derived from *p53−/−* and *p53R172H* knockin mice, transduced with control or oncogenic HRas-expressing retroviral vectors (Lang et al., 2004). As shown in Figure 4C, TGFβ induced the formation of the ternary complex between p63, mutant-p53 and Smads only in presence of oncogenic Ras (lane 4). Consistently, TGFβ promoted migration of MEFs in transwell assays only in cells expressing both mutant-p53 and oncogenic Ras (Figure 4D).

We previously showed that Ras promotes the formation of a complex between wild-type p53 and Smads by triggering phosphorylation the p53 N-terminus through CK1ε/δ kinases (Cordenonsi et al., 2007). We thus investigated whether a similar mechanism operated on mutant-p53. In breast MDA-MB-231 cells, endogenous oncogenic Ras is indeed required for mutant-p53 N-terminal phosphorylation (Figure S5A) and the formation of the TGFβ-induced ternary complex is inhibited by loss of Ras/MEK signaling or CK1ε/δ depletion (Figures 4E and S5B). Consistently, as shown in Figure S5C, mutation of the Ras/CK1-targeted phosphorylation sites of mutant-p53 abolished ternary complex formation in reconstituted H1299 cells (expressing oncogenic N-Ras, Table S1). In line with these biochemical data, Ras/CK1εδ signaling is required for TGFβ induced migration of MDA-MB-231 cells (Figure 4F) and p53R175H-reconstituted H1299 cells (Figure S5D). We finally

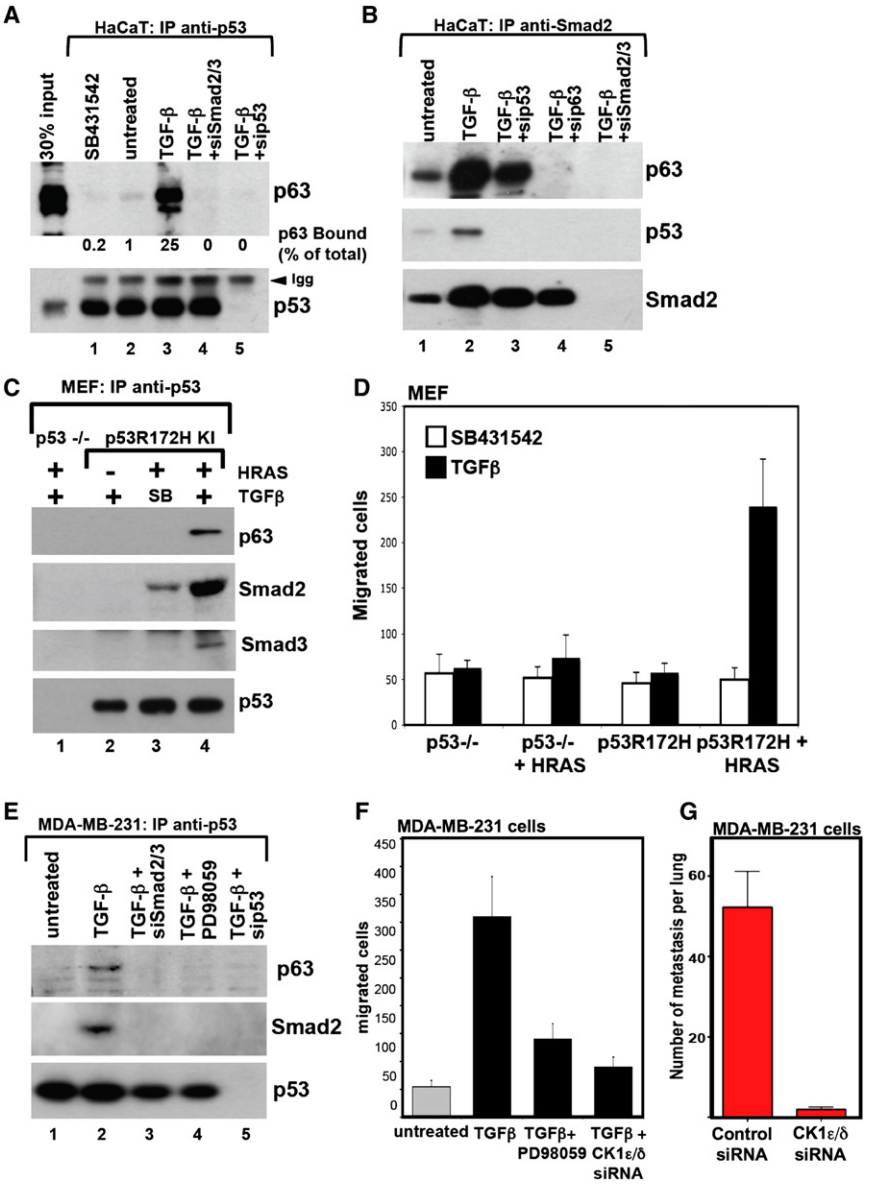

Figure 4. TGFβ and Ras Signaling Promote the Assembly of a Mutant-p53/Smad2/p63 Complex

(A) Co-immunoprecipitation/Western blot analysis of HACAT cell lysates showing endogenous p63 bound to mutant-p53 Cells were left untreated (lane 2) or treated for 1 hr either with 5 μM SB431542 (lane 1) or with TGFβ1 (5 ng/ml, lanes 3–5). Cells were transfected with anti-Smad2/3 (lane 4) or anti-p53 (lane 5) siRNAs two days before TGFβ treatment. The amount of p63 protein bound to mutant-p53 is shown as percentage relative to the amount of total p63 in the inputs.

(B) Western blot analysis of endogenous proteins: p63 and mutant-p53 coimmunoprecipitated with Smad2 from HACAT cell lysates.

(C) Mutant-p53 immunopurification from null or p53R172H knockin MEFs reveals the formation of a TGFβ- and Ras- dependent muant-p53/Smad/p63 endogenous ternary complex. Cells were transduced with empty vector (-) or G12V-HRas (+) and treated with the TGFβ receptor inhibitor SB431542 (SB) or with TGFβ1 (5 ng/ml).

(D) Transwell migration assays of MEFs with the indicated genotypes (as in C). Data are represented as mean and SD.

(E) RAS signaling enables ternary complex formation in MDA-MB-231 cells. Panels show Western blot analysis of p53 immunocomplexes from lysates of MDA-MB-231 left untreated (lane 1) or incubated for 1 hr with TGFβ1 (5 ng/ml) (lanes 2–5). p63 and Smad2 copurify with mutant-p53 in a TGFβ dependent manner (lanes 1 and 2). Mutant-p53 interaction with p63 is disrupted in cells depleted of Smad2 and Smad3 (lane 3) or when mutant-p53/Smad interaction is impaired by inhibiting the RAS pathway with PD98059 (lane 4). As specificity control, immunoprecipitations were carried out from p53-depleted cells (lane 5).

(F) The RAS/MEK/CK1εδ signaling pathway is required for TGFβ induced cell migration. The graph shows number of MDA-MB-231 cells migrated in a transwell assay. Cell migration in response to TGFβ1 is impaired by treatment with the MEK inhibitor PD98059 (60 μM) or by transfection with anti-CK1ε/δ siRNAs. Data are represented as mean and SD. Similar results were obtained by treating cells with the CK1ε/δ small molecule inhibitor IC-261 (data not shown, Cordenonsi et al., 2007).

(G) Lung colonization after tail vein injection of control and CK1ε/δ-depleted MDA-MB-231 cells (n = 10, 3 × 10^5 cells/mouse). Depletion was confirmed by western blotting (Figure S6). Data are represented as mean and SD.

validated in vivo the role of CK1ε/δ and found that CK1ε/δ-depleted MDA-MB-231 failed to undergo metastatic spread after tail vein injection in recipient mice (Figure 4G).

Together, data presented so far indicate that Ras/CK1 signaling enables ternary complex formation and empowers TGFβ-induced migration and breast cancer cell metastasis.

A Smad Bridge Allows Mutant-p53 to Oppose p63

Our evidences suggest that Smads serve as a critical bridge for the formation of an inhibitory complex between mutant-p53 and p63. Using immobilized GST-Smad3 and in vitro translated p63, we found that their interaction is direct (Figure 5A). Using different p63 isoforms, we dissected two independent Smad interaction surfaces in p63: the p63 N-terminal TA-domain contacts the MH1 domain of Smad3 whereas the p63 C-terminal alpha domain binds the Smad3-MH2 domain. While mapping Smad interaction in the TA domain confirms previous findings with p53 (Cordenonsi et al., 2007), the identification of a second Smad interaction surface in the alpha domain of p63 is interesting, first, because this domain has no structural counterparts in p53 and, second, because the vast majority of p63 is expressed in vivo as ΔNα isoform, lacking its TA-domain (Deyoung and Ellisen, 2007). These structural hints suggest that RSmad, by mean its N- and C-terminal domains may serve as a platform to assemble the mutant-p53/p63 complex (Figure 5B). This configuration might enable mutant-p53 to inhibit

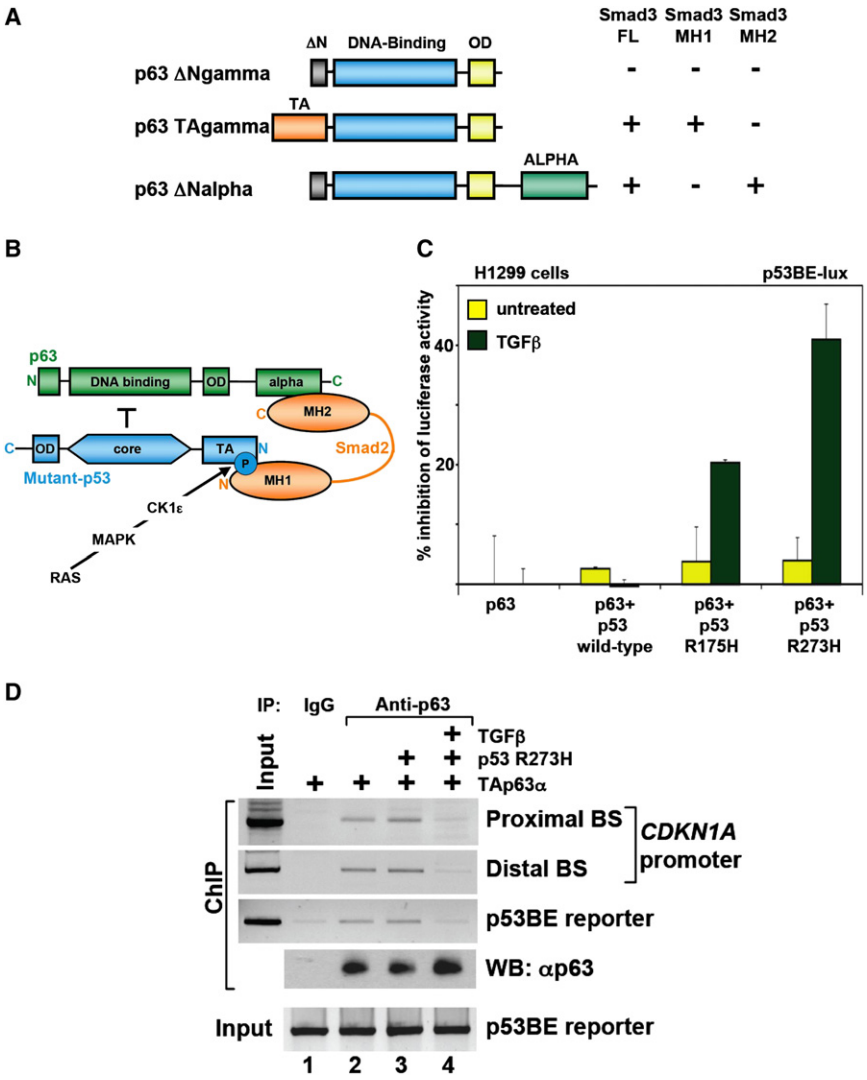

Figure 5. Smad Bridges Mutant-p53 to p63 Inhibition

(A) Panels show the summary of GST-pull down experiments using immobilized full-length Smad3 (Smad3 FL), Smad3-MH1-linker (Smad3 MH1) or Smad3-MH2-linker (Smad3 MH2) domains and in vitro translated p63 variants. We tested p63 isoforms corresponding to natural variants of this protein, bearing different domains at the N- and C terminus, as shown in the schematic representations of these molecules. See Figure S7 for raw data.

(B) Model for the ternary complex between ΔNp63α, Smad2 and mutant-p53.

(C) TGFβ signaling empowers the inhibition of p63 transcriptional activity by mutant-p53. H1299 null cells were transiently transfected with the p53BE-lux reporter and indicated p53/p63 expression vectors. Graphs show inhibition of the luciferase activity in cells cotransfected with p63 and *hp53R175H* or *hp53R273H* plasmids, coding for two distinct hot-spot mutant-p53 alleles. Wild-type p53 is uneffective. Data are represented as mean and SD. Importantly, additional mutations of p53 were tested with consistent results (Figure S8B).

(D) ChIP analysis of p63 bound to its cognate responsive elements of the endogenous *CDKN1A* promoter and transfected recombinant p53-BE-lux. H1299 cells were transfected with p63, mutant-p53 or constitutive-active TGFβ receptor expression vectors (TGFβ), as indicated. IgG in lane 1 are irrelevant total rabbit immunoglobulins, used as background control. p63 Western blotting ensures comparable pull-downs.

p63 transcriptional properties. To validate this hypothesis, we monitored p63 transcriptional activity in luciferase assays. p63 overexpression in H1299 cells potently induced transcription from the p53/p63 element of the *Mix.2* promoter (p53BE-lux) (Figure S8A). Cotransfection of several distinct mutant-p53 isoforms effectively inhibited p63 activity only in cells stimulated by TGFβ/Smad signaling (Figures 5C and S8B).

To better dissect the molecular mechanism of p63 repression we carried out ChIP analyses on the established p63 binding elements of the *CDKN1A* promoter (Deyoung and Ellisen, 2007). As shown in Figure 5D, binding of p63 to its cognate sites is quantitatively inhibited by mutant-p53 only in the presence of TGFβ signaling (lane 4). Similar results were obtained using transfected p53BE-lux reporter. Thus, incorporation of p63 into a TGFβ-induced ternary complex impairs p63 binding to DNA.

p63 Titration by Mutant-p53 and Smad Regulates Metastasis

During malignant progression, sequential elevations of TGFβ/Smad signaling is associated with the acquisition of metastatic potential (Cui et al., 1996; Oft et al., 2002). We thus explored the possibility that the metastatic shift of cancer cells could correspond to a quantitative inactivation of p63. For this, we monitored the dynamic of the trimeric complex in locally invasive D3 spindle carcinoma cells and their metastatic derivative D3S2, bearing constitutive Smad activity but expressing equal levels of p63, mutant-p53 (p53C236F) and oncogenic Ras (Oft et al., 2002; Table S1 and Figure 6A). Cell lysates were immunoprecipitated with anti-p53 antibodies and coprecipitating p63 quantified by Western blotting. The amount of p63 complexed by mutant-p53 raised dramatically upon TGFβ treatment in D3 cells (becoming 50% of the input), to become essentially quantitative (>95%) in metastatic D3S2 cells (Figures 6B and 6C). Thus, in advanced tumors, increasing doses of TGFβ/Smad2 signaling correspond to increasing levels of p63 trapped into mutant-p53-containing complexes.

D3S2 cells allow to validate in vivo the requirement of mutant-p53 and oncogenic Ras/CK1 signaling in a cellular context rendered metastatic by elevated Smad signaling (Figure S9A). As shown in Figure 6D, mutant-p53, high levels of oncogenic Ras and CK1ε/δ activity are required for lung metastasis of D3S2 cells upon tail vein injection in immunocompromised mice. This closely recapitulates our previous findings in human

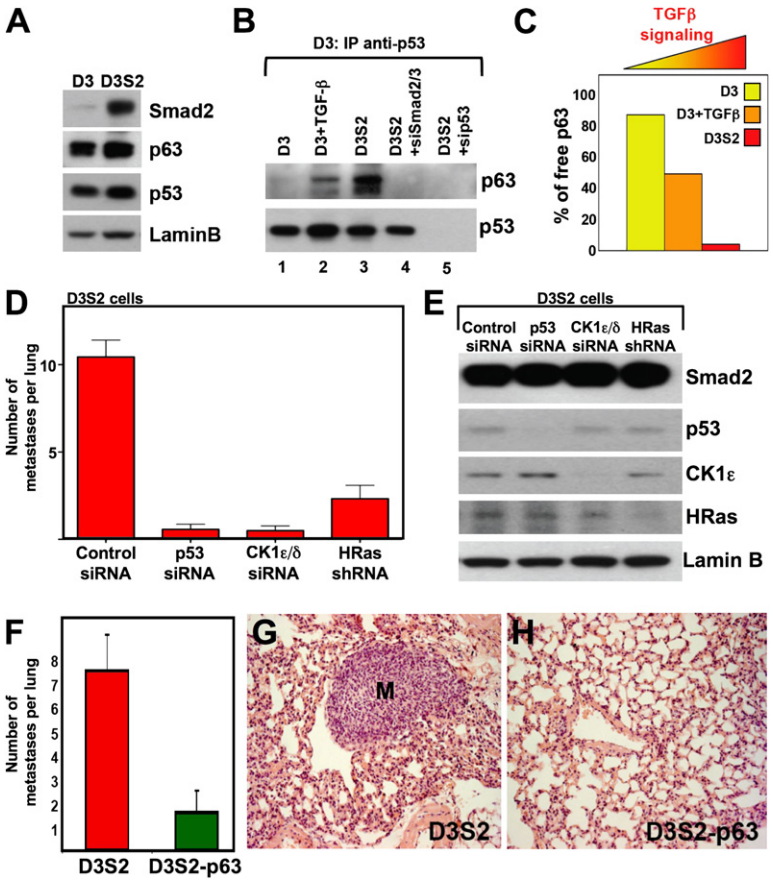

Figure 6. p63 Titration by Mutant-p53 and Smad Regulates Metastasis

(A) Western blot analysis of spindle cells D3 and their metastatic derivative D3S2 cells for Smad2, p63 and mutant-p53. p63 is detected after immunoprecipitation.

(B) Coimmunoprecipitation of p63 with mutant-p53 from D3 and D3S2 cell lysates. Increases in TGFβ signaling parallels with increasing incorporation of free p63 into ternary complexes (lanes 1-3). Complex formation is disabled after Smad2/3 knockdown.

(C) To quantify the fraction of free-p63 in the D3 series, we immunoprecipitated mutant-p53 and then quantified associated p63 by Western blot and finally compared this quantification to that one of the total p63 of the corresponding extract. The graph in the *y* axis indicated the remaining free p63.

(D and E) Lung colonization assay of control and mutant-p53-, CK1ε/δ- and HRas-depleted D3S2 cells after tail vein injection in SCID mice (n = 8–12 for each depleted cell population, 2×10^5 cells/mouse). See Figure S9C for representative photos of the corresponding lungs 25 days post-injection. Data are represented as mean and SD. When injected subcutaneously, control and siRNA-depleted cell population displayed comparable growth-rates (Figure S9B). (E) Panels show the corresponding immunoblotting.

(F–H) D3S2 or D3S2-p63 cells were injected as in (D) (n = 10 for each line, 2×10^5 cells/mouse). (F) Number of metastatic nodules in the lungs. Data are represented as mean and SD (G and H) Representative hematoxylin and eosin staining of lung sections from mice injected with D3S2 and D3S2-p63 cells; M, metastatic nodule.

breast cancer cells, suggesting a general impact for the mechanism here described in TGFβ-driven malignancy.

Further challenging the mutant-p53/p63 axis, we also tested in D3S2 whether tipping back the balance by raising p63 levels was sufficient to confer metastasis-protection. For this, we stably transduced D3S2 with ΔNp63α expression construct (D3S2-p63), and monitored lung colonization upon intravenous injection in recipient mice. D3S2-p63 cells displayed a remarkably weaker metastatic potential when compared to parental D3S2 (Figures 6F–6H). Notably, p63 expression did not impair tumor growth per se (Figure S9D). Thus, rebalancing the mutant-p53/p63 ratio specifically inhibits metastatic proclivity, underlining how even advanced cancer cells retain exquisite sensitivity to p63 activity.

A New Class of TGFβ Gene Responses

We next sought to investigate the specific gene expression program by which mutant-p53 and TGFβ control invasion and metastasis in breast cancer, for which a rich set of patients' databases with molecular profiles and associated clinical history is available.

We first compared the TGFβ transcriptomic profile of control and mutant-p53 depleted MDA-MB-231 cells. We found that TGFβ orchestrates the expression of a mutant-p53-independent genetic program entailing a large fraction of genes previously implicated in cell movement, invasion or metastasis (Figure 7A and Table S2); and yet, the phenotypic exploitation of this complex program occurs only in the presence of mutant-p53 (Figure 7B).

We therefore focused our attention to the much more restricted set of genes co-regulated by mutant-p53 and TGFβ; strikingly indeed, this entailed only five genes: *Sharp-1/DEC2/BHLHB3*, *Cyclin G2/CCNG2, ADAMTS9, Follistatin,* and *GPR87* (see table and northern blots in Figure S10). In particular, we focused on two, so far poorly characterized genes, *Sharp-1* and *Cyclin G2*, that are negatively regulated by TGFβ via mutant-p53: this suggested a role as metastasis suppressors (Figure 7C). To verify these molecules as positive targets of p63, control and p63 siRNA-depleted MDA-MB-231 cells were assayed for gene expression by quantitative RT-PCR. Loss of p63 potently inhibited the expression of *Sharp-1* and *Cyclin G2*, an effect phenocopied by TGFβ treatment in control cells (Figure 7D). Of note, TGFβ had no effect in p63 knockdown cells, suggesting that TGFβ has no additional, p63-independent, repressing effects on these genes.

Little is known on the transcriptional regulation of Sharp-1 or Cyclin G2. By means of ChIP, we identified in the *Cyclin G2* genomic region a binding element for endogenous p63 (Figure S11). In keeping with the requirement of mutant-p53 for TGFβ-mediated repression of these genes, we found that TGFβ antagonizes p63 recruitment to the *Cyclin G2* promoter in control MDA-MB-231 cells (Figure 7E, lanes 2 and 3) but failed to do so after mutant-p53 depletion (lanes 4 and 5).

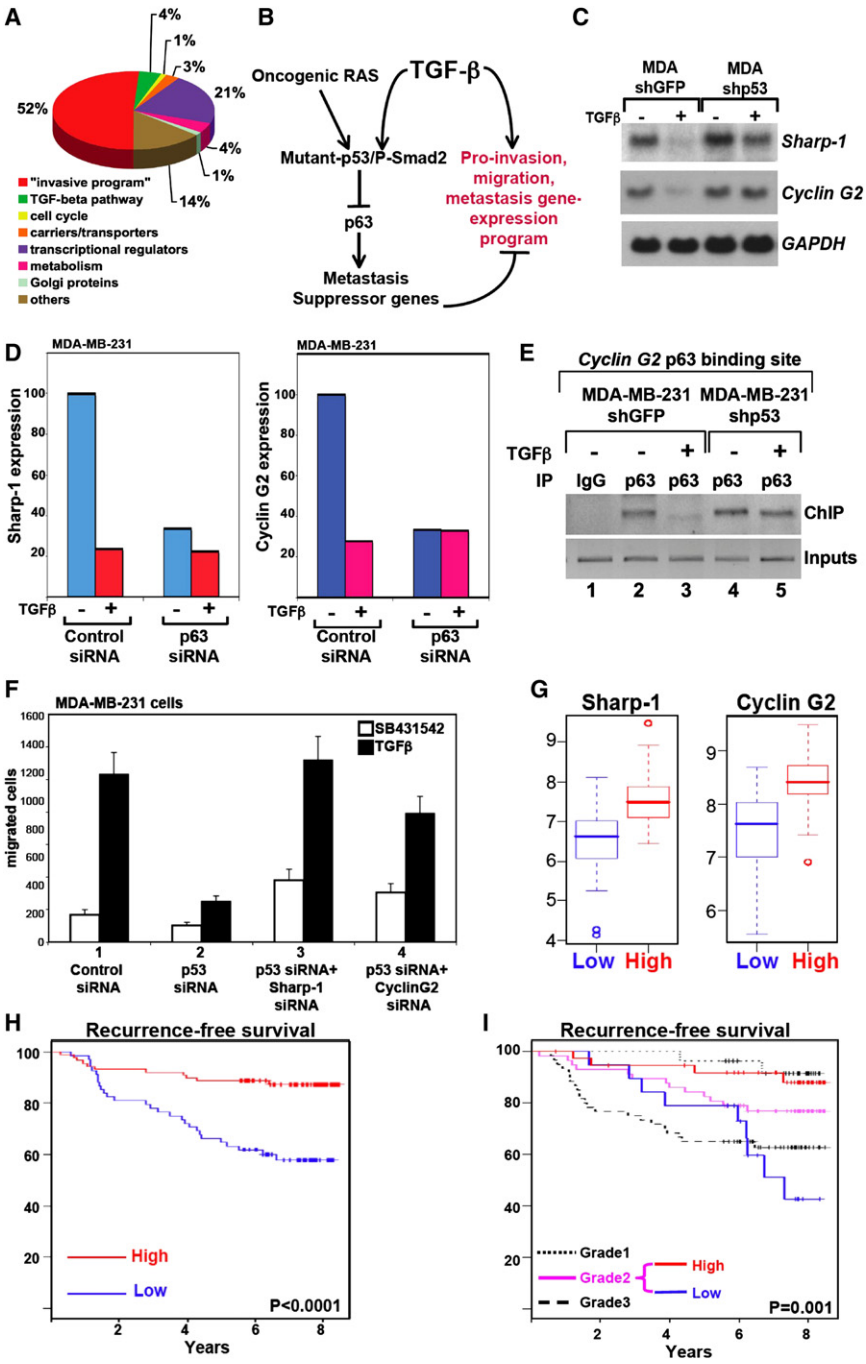

Figure 7. Identification and Clinical Validation of Candidate Metastasis Suppressors Downstream of the TGFβ /Mutant-p53/p63 Axis

(A) Overview of TGFβ target genes from microarray analysis of MDA-MB-231 cells. The graph shows functional classification for genes regulated by TGFβ in both MDA shGFP and MDA shp53 cell lines. Many genes codes for protein involved in cell invasion, migration and metastasis ("invasive program," see Table S2).

(B) Schematic representation of the dual role for TGFβ in promoting metastasis. TGFβ activates an invasive program independently of mutant-p53 expression. p63 restrains the deployment of this program by inducing metastasis suppressor genes. In mutant-p53 expressing cells, TGFβ can overcome this block by inactivating p63 through the mutant-p53/Smad2 axis.

(C) Regulation of Sharp-1 and Cyclin G2 expression by TGFβ and mutant-p53 in MDA-MB-231 cells. Northern blot analysis of MDA shGFP and MDA shp53 cells untreated or treated for two hours with TGFβ1 (5 ng/ml). GAPDH is a loading control. Both genes are downregulated by TGFβ in parental cells but not after mutant-p53 knockdown.

(D) *Sharp-1* and *Cyclin G2* are targets of endogenous p63 in MDA-MB-231 cells. Graphs show Sharp-1 and Cyclin G2 mRNA expression monitored by Q-PCR from cells transfected with control or anti-p63 siRNAs.

(E) ChIP analysis of endogenous p63 bound to its binding element in *Cyclin G2*. Lane 1 is a negative control ChIP carried out with aspecific rabbit IgG.

(F) The impairment of TGFβ-driven migration of mutant-p53 depleted cells in transwell assays can be rescued by concomitant depletion of Sharp-1 or Cyclin G2. Data are represented as mean and SD. For controls of effectiveness of independent siRNA sequences and knockdowns, see Figure S12.

(G, H and I) Analysis of the predictive power of the minimal signature (Sharp-1 + Cyclin G2).

(G) Statistical analysis of Sharp-1 and Cyclin G2 expression from the Stockholm dataset (including genomic data and matched clinical history for 156 patients). The analysis separates tumor samples in two groups, with coherent low or high expression of both genes, as visualized by box-plot graphs. "Low" and "High" are the names of the two groups of patients. Each box represents median and 75th and 25th percentile values.

(H) Kaplan-Meier graphs representing the probability of cumulative recurrence-free survival in breast cancer patients from the Stockholm dataset stratified according the minimal signature. The log-rank test p value reflects the significance of the association between minimal signature "High" and longer survival.

(I) Kaplan-Meier curves showing the recurrence free-survival for patients from the Stockholm dataset stratified according the Nottingham histological scale (grade 1 dotted line; grade 2, violet line; and grade 3, dashed line). Grade 2 tumors were further split in two groups by applying the minimal signature (red line: grade 2 and minimal signature high; blue line: grade 2 and minimal signature low). Notably, the "High" and "Low" groups displayed a recurrence-free survival rate similar to the grade 1 or grade 3 patients, respectively.

To functionally validate these genes as effectors of the mutant-p53/Smad/p63 pathway, we carried out epistasis experiments testing if depletion of Sharp-1 or Cyclin G2 could rescue TGFβ induced migration in p53-depleted cells. As shown in Figure 7F, siRNA-mediated knockdowns of Sharp-1 or Cyclin G2 restore TGFβ dependent promigratory activities in shp53 MDA-MB-231,

phenocopying p63-depletion. Thus, these molecules mediate the antagonizing effect of p63 on TGFβ proinvasive responses.

Clinical Validation of Sharp-1 and Cyclin G2

Having identified genes essential to antagonize invasive behavior in vitro, we then sought to elucidate their clinical relevance as metastasis suppressors. Recent transcriptomic profilings of primary human tumors have identified gene suites, or "signatures," that predict high risk of metastasis and poor disease-free survival (Fan et al., 2006). If the detection of Sharp-1 and Cyclin G2 in primary tumors is biologically meaningful, one might expect that reduced expression of these genes should be associated with poor clinical outcome. Of note, Sharp-1 and Cyclin G2 are not contained in known signatures for breast cancer metastasis, i.e., the "70-genes signature," the "recurrence score" or others (Fan et al., 2006).

To evaluate the prognostic value of Sharp-1 and Cyclin G2 (henceforth "minimal signature"), we took advantage of the available gene expression datasets summing up to 1200 primary breast cancers with associated clinical data, including survival and distant recurrence (Table S7). We defined in each dataset two groups of tumors with respectively high and low level of expression of Sharp-1 and Cyclin G2 (Figures 7G, S13, and S14) (see Experimental Procedures for statistical analyses). Strikingly, when tested using the univariate Kaplan-Meier survival analysis, the group expressing low levels of the minimal signature ("Low") displayed a significant higher probability to develop recurrence when compared to the "High" group (p values ranged from 0.02 to 3E-05, depending on the datasets) (Figures 7H, S13 and S14). Interestingly, the minimal signature performed comparably to the 70-genes profile in stratifying patients according to their clinical outcome (Figure S13) and is associated to risk of distant metastasis to both bone and lung (Figure S15).

To further evaluate the prognostic value of the minimal signature we performed multivariate Cox proportional-hazards analysis on the 187 tumors dataset from National Cancer Institute and 295 tumors from the NKI database (Fan et al., 2006; Sotiriou et al., 2006). With these cohorts, we could evaluate the minimal signature in the context of some variables commonly used in the clinical practice, such as estrogen-receptor status, tumor diameter, nodal status, tumor grade and treatment status. The minimal signature remained a significant predictor of metastasis-free survival (Tables S3 and S4). Furthermore, the minimal signature is an independent predictor of survival that adds new prognostic information to established clinical predictors such as size, node status, tumor grade, ER status, age and treatment (Figures S16 and S17). A point in case are tumors classified as intermediate (grade 2) by the Nottingham scale, that represent the majority of tumors and whose prognosis is uncertain (Ivshina et al., 2006). When applied to grade 2 tumors of multiple independent datasets, the minimal signature resolved these patients into two groups with outcomes comparable to grade 1 (good prognosis) and grade 3 (bad prognosis), respectively (Figure 7I and S18).

In sum, the clinical validation as prognostic tool of Cyclin G2 and Sharp-1, two targets of the TGFβ/mutant-p53/p63 axis, supports the general relevance of the mechanisms here described for breast cancer metastasis.

DISCUSSION

A TGFβ/Mutant-p53 Pathway for Metastasis

Here, we describe a signaling pathway that instills metastatic proclivity to epithelial cancer cells: TGFβ –> Smad/mutant-p53–| p63–| metastasis.

In this model, gain-of-TGFβ metastatic properties can be acquired by the combined action of two common oncogenic lesions, Ras and p53-mutation. Gain of mutant-p53 expression in noninvasive tumor cells empowers TGFβ proinvasive and migratory abilities, whereas loss of mutant-p53 expression in aggressive tumors impairs their metastagenicity.

A wealth of published data documented the requirement of Ras for TGFβ malignant responses but the mechanism of such interplay has not been addressed (Grunert et al., 2003). Our data provide a step forward in this direction: Ras signaling promotes mutant-p53 phosphorylation and, in so doing, it is required for the formation of the mutant-p53/Smad complex.

The critical role of mutant-p53 in metastasis has been recently suggested from elegant studies in transgenic mice, and this is particularly striking when expression of mutant-p53 is combined with oncogenic Ras (Caulin et al., 2007; Hingorani et al., 2005). In humans, p53 mutations are associated to poor prognosis in several types of tumors; intriguingly, p53-mutation is selected at very high frequency in aggressive HER-2 positive and basal-like breast cancers, that are particularly prone to metastasize (Sorlie et al., 2001).

How and when a tumor acquires metastatic properties is unknown (Bernards and Weinberg, 2002). Here we propose that mutations in the p53 and Ras pathways, selected to promote growth and survival of early neoplasms, also prefigure a cellular set-up with particular metastasis proclivity. This "passenger" trait will be exploited later on, during progression, to drive the metastatic switch, once cells gain access to high levels of TGFβ, either autonomously produced or extracted from the microenvironment.

p63 Opposes TGFβ-Induced Metastasis

We show a primary role for the p53 family member p63 as antagonist of TGFβ driven tumor invasiveness and metastasis. p63 is highly expressed in basal cells of stratified epithelia; however, its role during tumorigenesis is unclear (Deyoung and Ellisen, 2007). Here we show that functional inactivation of p63 by the TGFβ induced mutant-p53/Smad complex is critical for gain of metastatic proclivity. Mutant-p53 and Smad intercept p63 to form a ternary complex, in which the p63 transcriptional functions are antagonized. Thus, in presence of mutant-p53, TGFβ attains control over p63. This unleashes TGFβ malignant effects. Indeed, mutant-p53 knockdown in metastatic cancer cells does not affect the expression of the TGFβ invasive program but rather forestalls its phenotypic exploitation. As expected from p63 being downstream of mutant-p53, inactivation of p63 transforms non-invasive cells into malignant tumors and rescues metastasis ability in mutant-p53-depleted breast cancer cells. Moreover, the quantal increase of Smad signaling that renders metastatic D3 carcinoma cells coincides with a quantitative loss of "free," uncomplexed p63. Strikingly, tipping back the balance by adding

extra-p63 in these cells is sufficient to prevent such TGFβ-induced metastatic spread.

We previously showed that p53 family members and Smads cooperate for mesoderm development in *Xenopus* embryos and for growth arrest in mammalian cells, acting through independent binding elements in jointly-regulated promoters (Cordenonsi et al., 2003, 2007). Here we show that in metastatic cells p63 and TGFβ also play antagonistic functions. Indeed, in this context, Smads are not operating as transcription factors, but as adapters, bridging together mutant-p53 and p63.

What may then determine the predominance of tumor suppressive versus promalignant responses to TGFβ? We propose that a crucial determinant is the relative distribution of p63 into three pools: free, bound to Smad2 in transcriptionally cooperating complexes, or instead inactivated into mutant-p53/Smad2 ternary complexes. Mutation of p53, the levels of Ras and p63, as well as the strength of TGFβ signaling, are critical variables in p63 distribution. During tumor progression, sequential elevations of constitutive Ras and Smad2 activity would foster a more and more quantitative incorporation of p63 into ternary complexes. Beside dampening the growth arrest response, this would progressively titrate away the anti-metastatic properties of free-p63. Finally, in advanced stages of the disease, quantitative inactivation of p63 would finally unleash TGFβ-driven metastasis.

In this paper, we also tackled the issue of how p63 inhibits metastasis. We identified two genes, *Sharp1* and *Cyclin G2*, that are downstream of the TGFβ/mutant-p53/p63 pathway. These were functionally validated in vitro as essential mediators of p63-mediated antagonism toward TGFβ responses. Traditional prognostic markers are able to confidentially assign prognosis to less than 50% of breast cancer patients. For the rest of the patients, new prognostic tools are required to assess the risk of metastasis and thus identify those that would benefit from adjuvant treatments. Strikingly, in cancer patients, expression of Sharp-1 and Cyclin G2 represents a "minimal signature" with prognostic value independent from currently used clinical and histopathological variables. In spite of its simplicity, the minimal signature has predictive power comparable to more complex gene sets of predictors (Figure S13).

The mechanisms by which Sharp-1 and Cyclin G2 may act as metastasis suppressors in vivo remain ground for future studies. In the meantime, their use as diagnostic tools should be implemented for patients' stratification in the clinical laboratory.

EXPERIMENTAL PROCEDURES

Additional methods can be found in the Supplemental Data.

Transfections and Retroviral Infections

For siRNA transfection, dsRNA oligos (10 picomoles/cm^2) were transfected using the RNAi Max reagent (Invitrogen). A complete list of siRNAs is provided in Table S5. For transient overexpression studies, p63 expression vectors (0.4 μg/cm^2) were transfected in MDA-MB-231 using LT1 reagent (MIRUS). Wild-type and mutant-p53 expression constructs (7.5 ng/cm^2) were transfected in H1299 cells with Lipofectamine 2000 (Invitrogen).

Stable shRNA-expressing MDA-MB-231 cells were obtained by infection with pSuperRetro plasmids containing the interfering sequence (sh) indicated in Table S5 (as described in Dupont et al., 2009). Lentiviral vectors coding for wild-type-p53, mutant-p53 or p63DD were transfected in 293 cells in combination with pMDG and pCMV8.74 to obtain viral particles used to infect mutant-p53 depleted MDA-MB-231. D3S2-p63 were obtained by retroviral infection of D3S2 with pBABE-DNp63a. B9-p63DD and B9-GFP were obtained by retroviral delivery of p63DD-expressing or empty vector, respectively. Cells were drug selected to enrich for positive transfectants. MEFs were infected with a retroviral vector containing activated *H-RasG12V* cDNA and puromycin resistance as described in Lang et al., 2004.

Migration and Invasion Assays

For wound-closure experiments, H1299 cells were plated in 6-well plates and cultured to confluence. Cells were scraped with a p200 tip (time 0), transferred to low serum and treated as described. Number of migrating cells were counted from pictures (five fields) taken at the indicated time points.

Transwell assay were performed in 24 well PET inserts (Falcon 8.0 μm pore size) for migration assays and in Matrigel-GFR coated PET inserts (Falcon) for invasion assays. For MDA-MB-231, cells were plated in 10 cm dishes, transfected with siRNA or DNA plasmids and, after 8 hr, serum starved overnight. Then, 50000 or 100000 cells were plated in transwell inserts (at least 3 replicas for each sample) and either left untreated, treated with SB431542 (5 μM) or TGFβ1 (5 ng/ml). For H1299, cells were plated in the transwell in 10% serum but then changed to 0.2% serum. Cells in the upper part of the transwells were removed with a cotton swab; migrated cells were fixed in PFA 4% and stained with Crystal Violet 0.5%. Filters were photographed and the total number of cells counted. Every experiment was repeated at least three times independently.

For matrigel invasion assay shown in Figure S2C, MDA-MB-231 and derivative cell lines were resuspended in drops (100 μl) of Matrigel Growth Factor Reduced (BD Biosciences), diluted 1:2 in DMEM/F12.

In Vivo Metastasis Assays

Mice were housed in Specific Pathogen Free (SPF) animal facilities and treated in conformity with approved institutional guidelines (U.Padua and UCSF). For xenograft studies of breast cancer metastasis, shGFP- or shp53-MDA-MB-231 cells (1 x 10^6 cells/mouse) were unilaterally injected into the mammary fat pad of SCID female mice, age-matched between 5 and 7 weeks. After six weeks, mice were sacrificed and examined for metastases to lymph nodes. Macroscopic metastases to other organs were infrequent (liver, lung, peritoneum). Tumor growth in the injected site was monitored by repeated caliper measurements. For lung colonization assays, cells were resuspended in 100 μl of PBS and inoculated in the tail vein of SCID mice. Four weeks later, animals were sacrificed and lungs removed for the subsequent histological analysis. D3S2 and D3S2-p63 were also inoculated subcutaneously to evaluate the growth rate. The procedure for subcutaneous injection of mouse B9 squamous cancer cells was as previously described (Oft et al., 2002). For counting the total number of independent lesions per lung after tail vein injection, serial sections of the lungs, cut at a distance of 70 μm from each other, were stained with Hematoxylin and Eosin.

Protein Interaction Studies

To detect endogenous p63/Smad2/mutant-p53 complexes, cells were lysed by sonication in 20 mM HEPES (pH 7.8), 400 mM KCl, 5% Glycerol, 5 mM EDTA, 0.4% Np40, phosphatase and protease inhibitors, and cleared by centrifugation. For immunoprecipitations, extracts were diluted to 20 mM HEPES (pH 7.8), 50 mM KCl, 5% Glycerol, 2.5 mM MgCl2, 0.05% NP40 and incubated with the appropriate proteinA-sepharose bound antibodies for four hours at 4°C. Prior to IP, beads were incubated overnight in PBS with 2% BSA and 0.05% CHAPS. After three washes in binding buffer, copurified proteins were analyzed by immunoblotting by using as secondary antibodies the ExactaCruz reagents (Santa Cruz biotechnology) to reduce the background from IgG. The amount of coprecipitated p63 was determined by quantification of western blots using ImageJ (NIH). PAB421 monoclonal antibody (Calbiochem) was used for p53 immunoprecipitations. For Smad2 IPs, we used the anti-Smad2 polyclonal antibodies (S-20, Santa Cruz biotechnology). The procedure for GST-pull-down assays was described in Cordenonsi et al., 2003.

ACCESSION NUMBERS

Microarray data have been deposited in the Protein Data Bank with the accession number GSE14491.

SUPPLEMENTAL DATA

Supplemental Data include Supplemental Experimental Procedures, Supplemental References, eighteen figures, and seven tables and can be found with this article online at http://www.cell.com/supplemental/S0092-8674(09)00087-7.

ACKNOWLEDGMENTS

This work is dedicated to the memory of Stefano Ferrari. We thank O. Wessely, G. Bressan, D. Volpin, G. Del Sal, and all members of the Piccolo group for invaluable discussions and comments on the manuscript; G. Del Sal and J. Girardini for transgenic MEFs; L. Morsut for data-mining; A. Colombatti and P. Spessotto for training with transwell and invasion assays; G. Gallina for microarrays; and G. Blandino, L. W. Ellisen, M. Tripodi, and L. Naldini for gifts of reagents. C.W. is a Swiss National Science Foundation fellow. This work is supported by grants from Cariparo (Excellence grant) to S.B., from NCI (U01 CA84244) to A.B. and from the Italian Association on Cancer Research (AIRC) and Fondazione Cariparo (Excellence grant) to S.P.

Received: May 8, 2008
Revised: November 25, 2008
Accepted: January 13, 2009
Published: April 2, 2009

REFERENCES

Bernards, R., and Weinberg, R.A. (2002). A progression puzzle. Nature *418*, 823.

Caulin, C., Nguyen, T., Lang, G.A., Goepfert, T.M., Brinkley, B.R., Cai, W.W., Lozano, G., and Roop, D.R. (2007). An inducible mouse model for skin cancer reveals distinct roles for gain- and loss-of-function p53 mutations. J. Clin. Invest. *117*, 1893–1901.

Cordenonsi, M., Dupont, S., Maretto, S., Insinga, A., Imbriano, C., and Piccolo, S. (2003). Links between tumor suppressors: p53 is required for TGF-beta gene responses by cooperating with Smads. Cell *113*, 301–314.

Cordenonsi, M., Montagner, M., Adorno, M., Zacchigna, L., Martello, G., Mamidi, A., Soligo, S., Dupont, S., and Piccolo, S. (2007). Integration of TGF-beta and Ras/MAPK signaling through p53 phosphorylation. Science *315*, 840–843.

Cui, W., Fowlis, D.J., Bryson, S., Duffie, E., Ireland, H., Balmain, A., and Akhurst, R.J. (1996). TGFbeta1 inhibits the formation of benign skin tumors, but enhances progression to invasive spindle carcinomas in transgenic mice. Cell *86*, 531–542.

Derynck, R., Akhurst, R.J., and Balmain, A. (2001). TGF-beta signaling in tumor suppression and cancer progression. Nat. Genet. *29*, 117–129.

Deyoung, M.P., and Ellisen, L.W. (2007). p63 and p73 in human cancer: defining the network. Oncogene *26*, 5169–5183.

Dupont, S., Mamidi, A., Cordenonsi, M., Montagner, M., Zacchigna, L., Adorno, M., Martello, G., Stinchfield, M.J., Soligo, S., Morsut, L., et al. (2009). FAM/USP9x, a deubiquitinating enzyme essential for TGFbeta signaling, controls Smad4 monoubiquitination. Cell *136*, 123–135.

Fan, C., Oh, D.S., Wessels, L., Weigelt, B., Nuyten, D.S., Nobel, A.B., van't Veer, L.J., and Perou, C.M. (2006). Concordance among gene-expression-based predictors for breast cancer. N. Engl. J. Med. *355*, 560–569.

Flores, E.R., Sengupta, S., Miller, J.B., Newman, J.J., Bronson, R., Crowley, D., Yang, A., McKeon, F., and Jacks, T. (2005). Tumor predisposition in mice mutant for p63 and p73: evidence for broader tumor suppressor functions for the p53 family. Cancer Cell *7*, 363–373.

Gaiddon, C., Lokshin, M., Ahn, J., Zhang, T., and Prives, C. (2001). A subset of tumor-derived mutant forms of p53 down-regulate p63 and p73 through a direct interaction with the p53 core domain. Mol. Cell. Biol. *21*, 1874–1887.

Grunert, S., Jechlinger, M., and Beug, H. (2003). Diverse cellular and molecular mechanisms contribute to epithelial plasticity and metastasis. Nat. Rev. Mol. Cell Biol. *4*, 657–665.

Hingorani, S.R., Wang, L., Multani, A.S., Combs, C., Deramaudt, T.B., Hruban, R.H., Rustgi, A.K., Chang, S., and Tuveson, D.A. (2005). Trp53R172H and KrasG12D cooperate to promote chromosomal instability and widely metastatic pancreatic ductal adenocarcinoma in mice. Cancer Cell *7*, 469–483.

Ivshina, A.V., George, J., Senko, O., Mow, B., Putti, T.C., Smeds, J., Lindahl, T., Pawitan, Y., Hall, P., Nordgren, H., et al. (2006). Genetic reclassification of histologic grade delineates new clinical subtypes of breast cancer. Cancer Res. *66*, 10292–10301.

Lang, G.A., Iwakuma, T., Suh, Y.A., Liu, G., Rao, V.A., Parant, J.M., Valentin-Vega, Y.A., Terzian, T., Caldwell, L.C., Strong, L.C., et al. (2004). Gain of function of a p53 hot spot mutation in a mouse model of Li-Fraumeni syndrome. Cell *119*, 861–872.

Oft, M., Akhurst, R.J., and Balmain, A. (2002). Metastasis is driven by sequential elevation of H-ras and Smad2 levels. Nat. Cell Biol. *4*, 487–494.

Olive, K.P., Tuveson, D.A., Ruhe, Z.C., Yin, B., Willis, N.A., Bronson, R.T., Crowley, D., and Jacks, T. (2004). Mutant p53 gain of function in two mouse models of Li-Fraumeni syndrome. Cell *119*, 847–860.

Sobin, L.H., Wittekind, C., and International Union against Cancer. (2002). TNM classification of malignant tumours, 6th ed. (New York, Wiley-Liss).

Sorlie, T., Perou, C.M., Tibshirani, R., Aas, T., Geisler, S., Johnsen, H., Hastie, T., Eisen, M.B., van de Rijn, M., Jeffrey, S.S., et al. (2001). Gene expression patterns of breast carcinomas distinguish tumor subclasses with clinical implications. Proc. Natl. Acad. Sci. USA *98*, 10869–10874.

Sotiriou, C., Wirapati, P., Loi, S., Harris, A., Fox, S., Smeds, J., Nordgren, H., Farmer, P., Praz, V., Haibe-Kains, B., et al. (2006). Gene expression profiling in breast cancer: understanding the molecular basis of histologic grade to improve prognosis. J. Natl. Cancer Inst. *98*, 262–272.

Soussi, T., and Beroud, C. (2001). Assessing TP53 status in human tumours to evaluate clinical outcome. Nat. Rev. Cancer *1*, 233–240.

Strano, S., Fontemaggi, G., Costanzo, A., Rizzo, M.G., Monti, O., Baccarini, A., Del Sal, G., Levrero, M., Sacchi, A., Oren, M., et al. (2002). Physical interaction with human tumor-derived p53 mutants inhibits p63 activities. J. Biol. Chem. *277*, 18817–18826.